

# Direct quantification of the translocation activities of *Saccharomyces cerevisiae* Pif1 helicase

Chen Lu<sup>1,2</sup>, Shimin Le<sup>3</sup>, Jin Chen<sup>1</sup>, Alicia K. Byrd<sup>4</sup>, Daniela Rhodes<sup>5</sup>, Kevin D. Raney<sup>4</sup> and Jie Yan<sup>1,2,3,\*</sup>

<sup>1</sup>Mechanobiology Institute, National University of Singapore, Singapore 117411, <sup>2</sup>Centre for Bioimaging Sciences, National University of Singapore, Singapore 117557, <sup>3</sup>Department of Physics, National University of Singapore, Singapore 117542, <sup>4</sup>Department of Biochemistry and Molecular Biology, University of Arkansas for Medical Science, Arkansas 72205, USA and <sup>5</sup>School of Biological Sciences, Nanyang Technology University, Singapore 637551

Received February 23, 2019; Revised May 10, 2019; Editorial Decision June 04, 2019; Accepted June 07, 2019

## ABSTRACT

*Saccharomyces cerevisiae* Pif1 (ScPif1) is known as an ATP-dependent DNA helicase that plays critical roles in a number of important biological processes such as DNA replication, telomere maintenance and genome stability maintenance. Besides its DNA helicase activity, ScPif1 is also known as a single-stranded DNA (ssDNA) translocase, while how ScPif1 translocates on ssDNA is unclear. Here, by measuring the translocation activity of individual ScPif1 molecules on ssDNA extended by mechanical force, we identified two distinct types of ssDNA translocation. In one type, ScPif1 moves along the ssDNA track with a rate of  $\sim 140$  nt/s in 100  $\mu$ M ATP, whereas in the other type, ScPif1 is immobilized to a fixed location of ssDNA and generates ssDNA loops against force. Between the two, the mobile translocation is the major form at nanomolar ScPif1 concentrations although patrolling becomes more frequent at micromolar concentrations. Together, our results suggest that ScPif1 translocates on extended ssDNA in two distinct modes, primarily in a ‘mobile’ manner.

## INTRODUCTION

The Pif1 proteins are a group of DNA helicases belonging to the super family 1B, which have been found in all eukaryotes and some prokaryotes and viruses (1). The Pif1 proteins are implicated in a number of crucial chromosomal processes such as regulation of telomere and telomerase functions (2–4), resolution of R-loops formed during transcription (5), and processing Okazaki fragments (6). In addition to its DNA duplex unwinding activity that has been extensively studied (7–12), Pif1 proteins have also been shown able to unwind other nucleic structures such as

DNA–RNA hybrid and DNA G-quadruplexes (11,13–15), and remove proteins bound on ssDNA (16–18).

The DNA duplex unwinding activity of ScPif1 has been extensively investigated using both bulk and single-molecule assays on various DNA templates under different solution conditions (8,9,12,13). The DNA duplex unwinding activity implies that ScPif1 can likely translocate from 5' to 3' along ssDNA driven by chemical energy from ATP hydrolysis. Indeed, the ssDNA translocation activity was inferred in several bulk studies (9,17) and more recently in single-molecule Förster resonance energy transfer (smFRET) studies (11,18). Based on the high resolution data from smFRET studies, an ssDNA patrolling activity of ScPif1 was proposed as the mechanism underlying its translocation on ssDNA. Briefly, ScPif1 is tightly anchored at an ssDNA/dsDNA junction, while the translocation domain of the ScPif1 is free to travel along the ssDNA with a 5' to 3' directionality. The translocation domain dissociates from the ssDNA track after it reaches the end, but resumes the patrolling whenever bound on ssDNA again, generating an ssDNA loop in a repetitive manner (11,18). However, bulk assays of ScPif1 translocation have used ssDNA templates which do not contain an ssDNA/dsDNA junction. Whether ScPif1 patrols on ssDNA and the necessity of an ssDNA/dsDNA junction for this activity remain unknown.

In order to provide new insights into how ScPif1 translocates on ssDNA, we developed a label-free single-molecule assay. We specifically addressed a question concerning whether ScPif1 translocation requires anchoring/immobilizing itself to an ssDNA/dsDNA junction, or whether it could move along an ssDNA track in a mobile manner. On ssDNA extended by mechanical force, we observed that (i) ScPif1 could translocate along ssDNA track in a mobile manner, (ii) ScPif1 could also patrol on ssDNA without any ssDNA/dsDNA junction, which results in generation of ssDNA loops during translocation, (iii) the patrolling mode of translocation is rare in nM concentration range of ScPif1, whereas its occurrence

\*To whom correspondence should be addressed. Tel: +65 6516 2620; Email: phyjy@nus.edu.sg

becomes frequent when the concentration of ScPif1 was increased to  $\mu\text{M}$  range.

## MATERIALS AND METHODS

### Single-molecule magnetic tweezers

A home-built back-illuminated magnetic tweezers setup (19) was used in this study and bead height was measured at a spatial resolution of  $\sim 2$  nm and temporal resolution of 100 Hz. For a given superparamagnetic bead tethered to a molecule, the force is solely dependent on the bead-magnet distance  $d$ . A standard force–distance curve  $F_0(d)$  had been generated using multiple test beads over a range from 1 to 100 pN (19). The force applied to any other bead placed at the same bead-magnet distance  $d$  differs from the standard curve by a force-independent factor  $\gamma$  that varies from one bead to another (19,20). Therefore, if one can determine the value of  $\gamma$  of a bead, the force applied to the bead at any other bead-magnet distance  $d$  can be calculated by extrapolation using the standard curve,  $F(d) = \gamma F_0(d)$ . In this study, the value of  $\gamma$  is determined at a value of  $d$  where force-dependent DNA overstretching transition in 1 M NaCl corresponds to  $68 \pm 0.9$  pN (21). Therefore, the force calibrated using this method has a relative error of  $<2\%$ . Further details of generating the standard force–distance curve and force calibration can be found in our previous publications (19,20).

### DNA construction

A 630-nt ssDNA was used for the patrolling assay, which was generated from an original 630-bp dsDNA through force-dependent strand separation transition at  $\sim 65$  pN in 100 mM NaCl (22). The 5' and the 3' ends of the same ssDNA strand in the original dsDNA were labelled with biotin and azide respectively. The biotinylated end is tethered to a streptavidin-coated superparamagnetic bead (Dyna-beads M-280, Thermo Fisher Scientific) and the azide-labelled end was attached to an alkyne-coated coverslip through click chemistry (23). After the force-dependent strand separation transition, the unlabeled strand dissociates and diffuses away, leaving the tethered strand under force. The dual-hairpin construct used for the mobile translocation assay was similarly produced by force-dependent strand separation transition from an original dsDNA and tethered through biotin/streptavidin and click chemistry approach. The original dsDNA contains two pairs of palindromic sequences; therefore, after conversion into ssDNA, two hairpins can form at low forces. Further details of producing these DNA constructs and the click chemistry can be found in Supplementary Information Text S1.

### Determination of mobile translocation rate

Mobile translocation rate was calculated by dividing  $\Delta n$ , the number of nucleotides of ssDNA track exposed when AT-rich hairpin fully unzipped by force increase, by  $\Delta t$ , the time between force increase and unzipping of the GC-rich hairpin.  $\Delta t$  was directly measured in experiment, while

the value  $\Delta n$  was calculated based on total number of nucleotides in the AT-rich hairpin region subtracting the number of nucleotides that ScPif1 already traveled before the force increase. Briefly, when the unwinding of the AT-rich hairpin was observed at  $\sim 12$  pN, an extension increase of  $\Delta x$  (shown in Figure 3 A) was recorded. Then force was jumped to 17 pN to expose the remaining nucleotides in the AT-rich hairpin, creating an ssDNA track for ScPif1 to translocate. The number of nucleotides created in the track  $\Delta n$  can be estimated by  $208 - 0.5 * \Delta x / x_{ss}^{1nt}$ , where 208 is the total number of nucleotides in the 100-bp hairpin plus the 4-nt end loop and the 4 nt linker between the AT-rich and GC-rich hairpins.  $x_{ss}^{1nt}$  is the force-extension curve of ssDNA per nucleotide, which was approximated using the Marko-Siggia formula (33) assuming the worm-like chain polymer model of ssDNA. The worm-like chain polymer model has been shown able to fit the ssDNA force-extension data obtained over a wide range of solution conditions (32), which is also confirmed in our reaction solution condition (Supplementary Figure S1).

### Quantification of patrolling activity

Quantification of loop generating activity was performed semi-automatically via a home-written script on the Igor Pro 6.0 platform (Wavemetrics). The looping event was counted only if three criteria were met: (i) the loop size was larger than 5 nm; (ii) the time span of looping event was larger than 0.5 second; (iii) the rate of extension decrease was larger than 0.5 nm/s. Loop sizes and loop rates were converted to the unit of nt and nt/s, using force-extension curve of ssDNA in our experimental buffer condition (Supplementary Figure S1).

## RESULTS

In order to investigate how ScPif1 translocates along ssDNA, we designed three different constructs that can be used to probe mobile translocation and patrolling activities of ScPif1. Figure 1A shows a double-hairpin construct to probe mobile translocation. It contains two neighbouring DNA hairpins, a 5' AT-rich hairpin and a 3' GC-rich hairpin. The principle of the measurement is as follows—when ScPif1 dependent unwinding of the AT-rich hairpin is detected near the fork entry, force is jumped to a value higher than the threshold force of unfolding the AT-rich hairpin but below that of the GC-rich hairpin. This will cause immediate unzipping of the AT rich DNA hairpin, creating an ssDNA track for the ScPif1 molecule to translocate. The number of nucleotides of the ssDNA track created ahead of the ScPif1 can be calculated based on the force-extension curve of ssDNA (Materials and Methods). When the ScPif1 reaches the fork entry of the GC-rich hairpin, it begins to unwind the hairpin. The rate of translocation can be calculated as the number of translocated nucleotides divided by the time taken for the ScPif1 to reach the GC-rich hairpin. Figure 1B and C shows constructs used to probe the patrolling of ScPif1. Two possible scenarios are considered: (i) ScPif1 is immobilized to an ssDNA/dsDNA junction (Figure 1B) during translocation and (ii) ScPif1 is immobilized to an ssDNA site during translocation (Figure 1C). In both

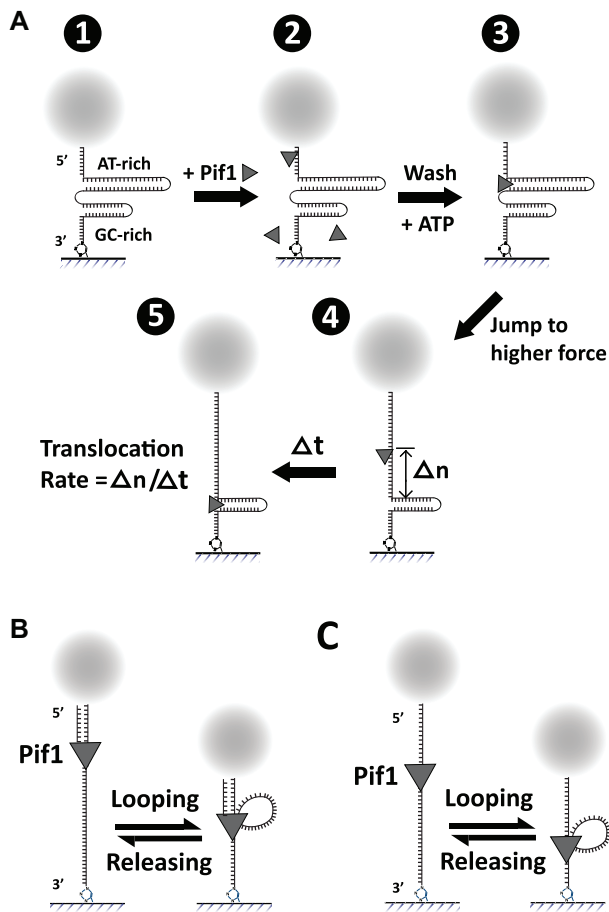


**Figure 1.** Single-molecule assay for translocation of ScPif1. (A) The schematic illustration of the assay using a double-hairpin construct comprising an AT-rich hairpin and a GC-rich hairpin linked by a 4-nt poly-T linker (A-1). At a low force under which both hairpins are zipped, ScPif1 is loaded at the 5' end ssDNA handle (A-2), and is activated after excessive wash and introducing ATP (A-3). After unwinding of the AT-rich hairpin is observed, the AT-rich hairpin is mechanically unzipped while the GC-rich hairpin remains zipped, creating an ssDNA track of certain number of nucleotides,  $\Delta n$ , for the ScPif1 translocates (A-4). The time taken till unwinding of the GC-rich hairpin,  $\Delta t$ , is recorded, from which the translocation rate is calculated by  $\Delta n/\Delta t$  (A-5). (B and C) Designs for probing the patrolling of ScPif1 in the presence (B) or absence (C) of ssDNA/dsDNA junction.

scenarios, the translocation is expected to generate a downstream ssDNA loop.

### ScPif1 undergoes mobile translocation

Using the double-hairpin construct (Figure 1A), we investigated the translocation speed of ScPif1. Besides the ~630-nt ssDNA handles at both ends, the construct contains a 5' 100-bp AT-rich hairpin (72% AT) and a 3' 50-bp GC-rich hairpin (66% GC), separated by 4-nt poly-T loop. Due to the big difference in the AT/GC ratio between the two hairpins, they unzip at well-separated force ranges in our buffer solution condition (50 mM KCl, 5 mM MgCl<sub>2</sub>, 10 mM Tris, 1 mM DTT, pH 7.4) (Figure 2). The AT-rich hairpin can be instantly unzipped by applying a force of  $17.0 \pm 0.3$  pN

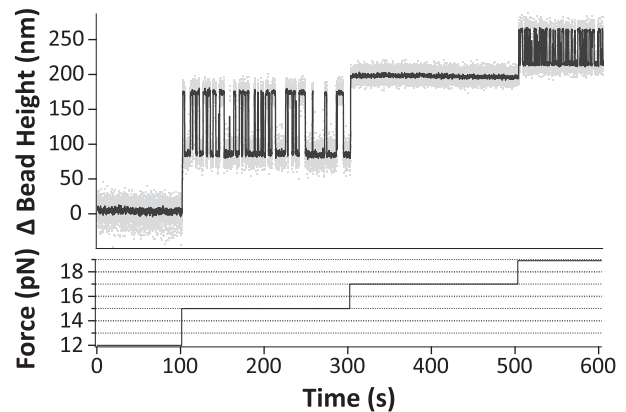


**Figure 2.** Characterization of the double-hairpin construct. The data show a representative time trace of the bead height change at four different forces of  $12.0 \pm 0.2$ ,  $15.0 \pm 0.2$ ,  $17.0 \pm 0.3$  and  $19.0 \pm 0.3$  pN. In our buffer condition, the critical unzipping forces for the AT-rich and GC-rich hairpins are around 15 and 19 pN, respectively. At force of  $17.0 \pm 0.3$  pN, the AT-rich hairpin is completely unzipped while the GC-rich hairpin remains completely zipped.

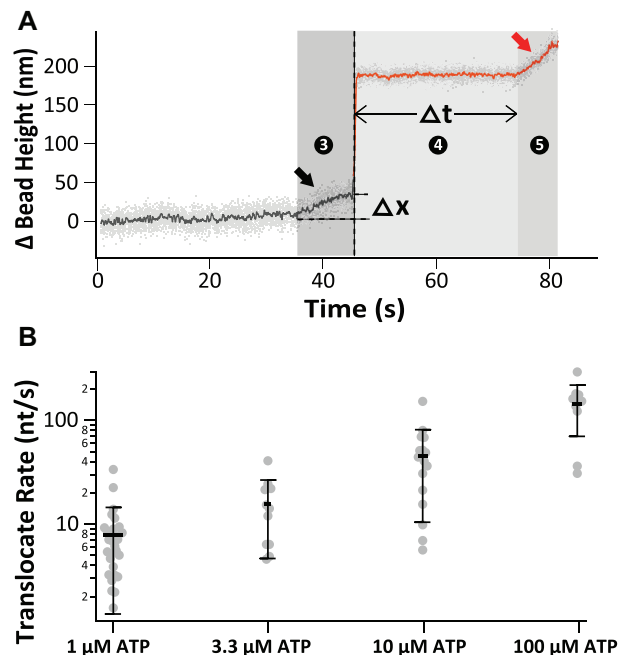


**Figure 3.** Mobile translocation assay of ScPif1. (A) The panel shows a representative time trace of the bead height change of the double-hairpin construct during the action of an ScPif1 molecule in  $3.3 \mu\text{M}$  ATP. The tether was initially held at a force of ~12 pN (gray data in the first 45 s). When unwinding of the AT-rich hairpin was observed (black arrow), force was jumped to ~17 pN to unzip the AT-rich hairpin. The tether was held at the force until the unwinding of the GC-rich hairpin was observed (red data in 45-81 s; unwinding is indicated by red arrow). (B) Scatter dot plot of the mobile translocation rates of ScPif1 (mean and standard deviations) measured at different ATP concentrations.

at which the GC-rich hairpin remains stable, and it can be instantly rezipped after jumping back to ~12 pN (Supplementary Figure S2).

After characterization of the double-hairpin construct, 5 nM ScPif1 was introduced in the absence of ATP. ScPif1

can bind the two ssDNA overhangs, but only the one bound at the 5' overhang adjacent to the AT-rich hairpin can translocate in 5' to 3' direction (Figure 1A). As ScPif1 occupies a minimum size of 6-8 nt ssDNA (25,29), the 4-nt poly-T loop between the hairpins is expected not to be able to load ScPif1. After incubating for a few minutes, free ScPif1 was washed away using 300  $\mu$ L buffer solution (Supplementary Figure S3), followed by introducing solution containing various concentrations of ATP. Figure 3A shows a representative time trace of the bead height recorded during an experiment. After observing unwinding activity of the AT-rich hairpin indicated by an extension increase of  $\Delta x$  (the first black arrow) at a force of  $\sim 12$  pN (data in black), the force was jumped to  $\sim 17$  pN, which caused immediate unzipping of the AT-rich hairpin while keeping the GC-rich hairpin folded. After the force jump, the new bead height (data in red) remained at a nearly constant level for  $\Delta t \sim 25$  s before unwinding of the GC-rich hairpin was observed (red arrow). After jumping force back to 12 pN, we found that the AT-rich hairpin could rezip and the same ScPif1 could remain associated and relocate to the entry of the AT-rich hairpin (Supplementary Figure S4). This allowed us to repeat the force-jump procedure to obtain multiple data for each ScPif1 before it completely dissociated or lost the activity.

Applying the above assay for more than twenty independent tethers (more than three at each ATP concentration), we obtained the ssDNA translocation rate of ScPif1, which is the number of nucleotides traveled, in different ATP concentrations up to 100  $\mu$ M, as shown in Figure 3B. The data show that the translocation rate increases as the ATP concentration increases, reaching 140 nt per second when ATP concentration tops at 100  $\mu$ M. At ATP concentrations higher than 100  $\mu$ M, after force-jump to  $\sim 17$  pN, the time taken to unwind the GC-rich hairpin ( $\Delta t$ ) became too short ( $< 1$  s) to be accurately determined using our assay. While the ATP concentration range does not allow us to measure the maximal translocation rate at saturating ATP concentration, we tried to estimate it based on fitting the data using Michaelis–Menten equation  $V_{\text{translocation}} = V_{\text{max}}[\text{ATP}]/(K_M + [\text{ATP}])$ , where  $K_M$  and  $V_{\text{max}}$  are the Michaelis–Menten constant and maximal translocation rate, respectively. Due to the limited number of data points at each ATP concentration, and the below-saturation concentration range of ATP used in these measurements, large statistical uncertainties of the best-fitting values of  $K_M$  and  $V_{\text{max}}$  are expected, which are estimated based on bootstrap analysis (Supplementary Figure S5 caption). Such data fitting and statistical analysis led to the following estimated values of  $V_{\text{max}} = 222.0 \pm 152.5$  nt/s and  $K_M = 44.3 \pm 53.5$   $\mu$ M (Supplementary Figure S5).

Together, these results clearly indicate that ScPif1 can translocate along ssDNA track in a mobile manner at fast rates. We note that once the unwinding activity of the AT-rich hairpin was observed, there is about 85% of chance (in 67 out of 79 total events) to observe the delayed unwinding of the GC-rich hairpin after the AT-rich hairpin was mechanically unzipped, indicating that some of the ScPif1 helicases could dissociate before they reached the GC-rich hairpin.

### ScPif1 can also undergo patrolling on ssDNA

Besides the mobile translocation, we also observed patrolling of ScPif1 on ssDNA in a similar concentration range (5-20 nM) where the mobile translocation was observed. In this mode, on ssDNA without any ssDNA/dsDNA junction (Figure 1C), repetitive ssDNA shortening and extending cycles with large amplitude were observed over a wide range of forces. Each cycle contains a gradual shortening stage and a following abrupt extending step (Figure 4A for several representative time traces). The phenomenon is dependent on ATP hydrolysis, as it was not observed in 100  $\mu$ M ADP or in 100  $\mu$ M AMP-PNP. In this ScPif1 concentration range, the occurrence of this mode of translocation is much rarer than the mobile translocation mode. However, once repetitive ssDNA shortening and extending were observed, it could last for minutes to tens of minutes after removing free ScPif1 in solution (Figure 4B for a representative time trace). Therefore, such phenomenon is not due to binding/unbinding of ScPif1 to ssDNA.

Such ATP-dependent activity of ScPif1 on ssDNA could be most logically explained by a patrolling mode of ScPif1, where a domain on ScPif1 is anchored to a site on ssDNA while its motor domain translocates. As schematized in Figure 1B and C, this mechanism would lead to ssDNA looping that causes processive extension decrease against force. In addition, stochastic disengagement of the motor domain from ssDNA could explain the abrupt extension increase. Cycles of engagement and disengagement between the motor domain of the same tightly bound ScPif1 and ssDNA can explain the observed repetitive shortening and extending of ssDNA in the absence of free ScPif1 in solution.

This ssDNA-looping activity of ScPif1 was observed over a wide range of force up to 50 pN (Figure 4A). The number of nucleotides absorbed into the ssDNA loop during each looping activity until the abrupt extending step can be estimated from the extent of extension decrease based on the worm-like chain polymer model of ssDNA using the Marko-Siggia formula (33). Data obtained from three to six independent tethers at each force are represented using scatter-dot plot (mean with standard deviation) (Figure 4C, top panel). The results show that the loop size reduces as force increases. Similarly, the looping rate, which is the number of nucleotides absorbed into the ssDNA loop per second, can be converted from the measured speed of extension decrease during loop formation. The scatter dot plot representation (Figure 4C, bottom panel) also shows that the looping rate decreases as force increases.

The observed repetitive ssDNA looping and releasing phenomenon is much rarer than the mobile translocation. Within our typical experimental time scale of 2–3 h, in 5–20 nM ScPif1 solution, such phenomenon was observed in  $< 10\%$  of total number of independent experiments (more than 100). In this concentration range, the mobile translocation occurred almost immediately after flowing ScPif1 in the presence of above- $\mu$ M ATP. Therefore, binding of ScPif1 to ssDNA in the presence of ATP is insufficient for the patrolling to occur. Experiments were repeated on the same ssDNA annealed with a 32-nt complementary oligo at the 5' end (Figure 1B); however, the occurrence probab-

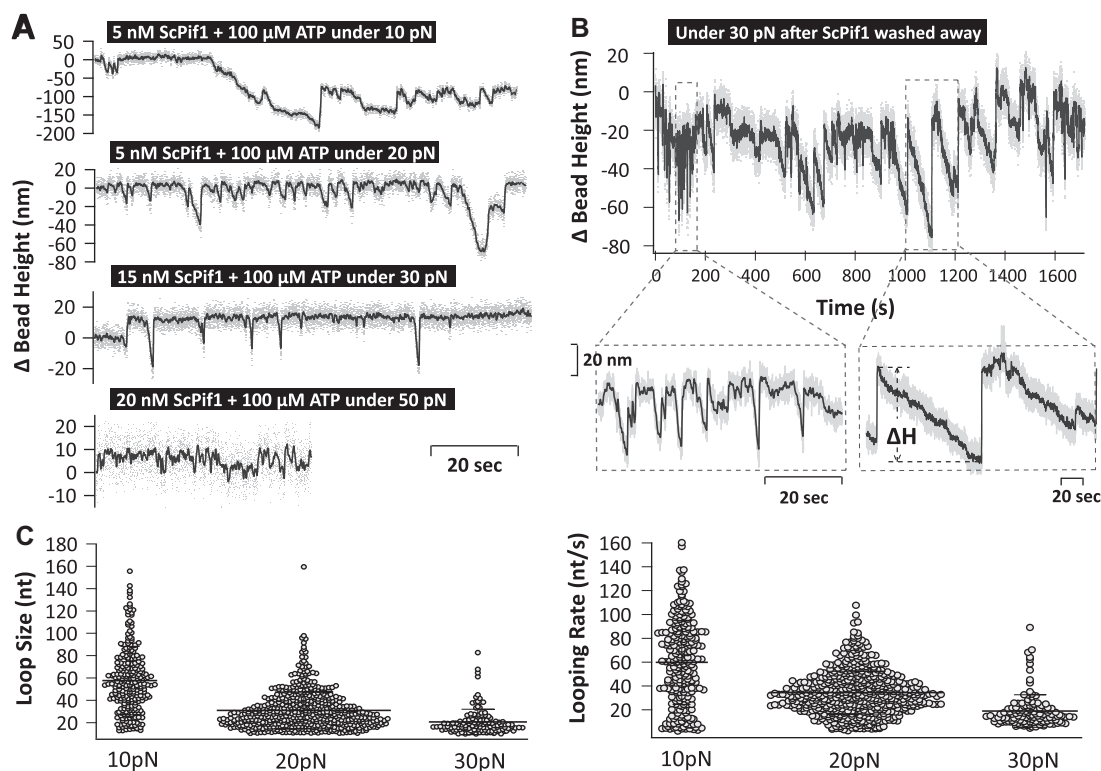


**Figure 4.** Patrolling activities of ScPif1. (A) Four representative time traces of bead height recorded at different forces up to 50 pN from four independent tethers in 5–50 nM ScPif1 and 100  $\mu$ M ATP, which show repetitive patrolling signals. (B) The panel shows a representative time trace of the bead height change recorded at  $\sim 30 \pm 0.5$  pN during patrolling of ScPif1 in 1 mM ATP on a 630-nt ssDNA after removal of free ScPif1. Two zoomed-in regions are provided to give finer details of the repetitive translocation signals. (C) The looping sizes (left panel) and looping rates (right panel) against three different stretching forces were summarized in scatter dot plots (mean and standard deviation).

ity was not significantly increased. On the other hand, once emerged, it could last for up-to-tens-of-minutes even after removal of free ScPif1 (Figure 4B). Together, these results suggest that the patrolling activity likely results from a rare species of ScPif1 which might bind ssDNA with a low off-rate and produces long duration of repetitive translocation activity.

While the nature of this rare species remains obscure, we consider both an oligomerization state of the ScPif1 and a rare binding mode of ScPif1 to ssDNA as the potential candidate. In either case, higher concentration of ScPif1 should be able to increase the occurrence probability of the patrolling events. Therefore, we increased the concentration of ScPif1 to 1  $\mu$ M ScPif1 at 100  $\mu$ M ATP. In seven of ten independent experiments, within 30 minutes we observed obvious repetitive shortening and extending behaviors (Figure 5A). These repetitive shortening and extending behaviors in  $\mu$ M ScPif1 were dependent on ATP, as they were not observed in the absence of ATP (Supplementary Figure S6).

Interestingly, the amplitude of the patrolling activity observed in  $\mu$ M ScPif1 is much smaller than that observed at low ScPif1 concentrations. Such small amplitude also made it difficult for quantification of the amplitude and looping rate. We reasoned that the much smaller amplitude of looping is likely caused by obstacles of abundantly and tightly bound ScPif1 on ssDNA, which restricts the translocation range of the motor domain of the loop-generating ScPif1 species. It has been shown that nucleotide induces weaker

binding of ScPif1 to ssDNA (24). We reasoned that by increasing the turnover rate of ScPif1 at higher ATP concentration, the bound ScPif1 may become more dynamic and thus permit more persistent motion of the loop-generating ScPif1 species. Indeed, in 1  $\mu$ M concentrations of ScPif1 and 1 mM ATP, repetitive patrolling behaviours with faster looping rate and larger amplitude than those in 100  $\mu$ M ATP were observed in every experiment of >10 independent experiments within 10 min after ScPif1 solution was introduced (Figure 5B for four representative time traces).

Together, these results suggest that there exists a species of ScPif1 that can induce the patrolling mode of translocation on ssDNA without an ssDNA/dsDNA junction. The concentration of this species increases as ScPif1 concentration increases, and its activity on ssDNA is restricted by the dynamics of other proteins bound on ssDNA. This patrolling mode of translocation on ssDNA was not caused by ScPif1 non-specifically absorbed on the bead surface attached to the 5' end of ssDNA, as the same activity was observed when a long PEG linker was added between the 5' end of the ssDNA and the bead (Supplementary Figure S7).

## DISCUSSION

In summary, in this work we investigated the ssDNA translocation activity of ScPif1 using magnetic tweezers. We identified two distinct modes of translocation on ssDNA ex-

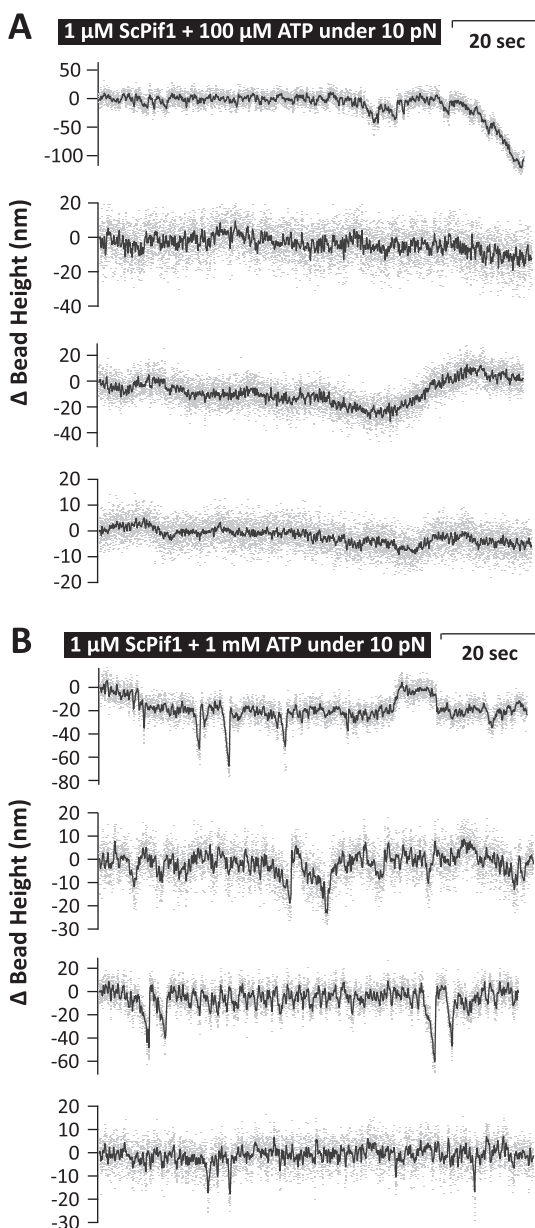


**Figure 5.** Patrolling activities at high concentration of ScPif1. (A) Four representative time traces of bead height recorded at  $10 \pm 0.2$  pN from four independent tethers in  $1 \mu\text{M}$  ScPif1 and  $100 \mu\text{M}$  ATP. (B) Four representative time traces of bead height recorded at  $10 \pm 0.2$  pN from four independent tethers in  $1 \mu\text{M}$  ScPif1 and  $1 \text{mM}$  ATP.

tended by mechanical force, which we have referred to as the mobile translocation and patrolling. In the mobile translocation mode, an ScPif1 molecule moves along an ssDNA track without anchoring itself to a fixed point on the ssDNA. In contrast, in the patrolling, a domain on ScPif1 is anchored to a fixed site on ssDNA, while in the meantime the motor domain translocates on ssDNA resulting in generation of large ssDNA loops.

While the mechanism underlying the two distinct modes of the ssDNA translocation of ScPif1 remains unknown, it might indicate multiple modes of ScPif1 interacting with ssDNA. It has been shown that ScPif1 exists as a monomer in

solution with a molecular weight of  $\sim 98$  kDa (7). Bound on ssDNA, on average an ScPif1 occupies a size of 6–8 nt (25,29). However, under excess ratio of ScPif1 to available ssDNA binding sites, strong evidences have suggested that ScPif1 dimerizes (25) or forms higher order oligomers (9,14) upon binding to ssDNA. Since the occurrence of the patrolling mode significantly increased when the concentration of ScPif1 was increased from nM range to  $\mu\text{M}$  range, it is likely that the patrolling mode is related to oligomerization state of ScPif1, though other possibilities like a unique binding mode of ScPif1 to ssDNA cannot be ruled out.

In the mobile translocation mode, using a novel double-hairpin assay, the rate of translocation was measured to be  $\sim 140$  nt/s at  $100 \mu\text{M}$  ATP on ssDNA extended by  $\sim 17$  pN. This is not the saturated translocation rate, as when we increased the ATP concentration, the translocation rate further increased to a level that cannot be quantified accurately by our instrumentation. However, this value is already higher than the values (typically  $< 100$  nt/s) estimated in previous bulk assays (9,17) and smFRET assays (11,18) measured at a much higher ATP concentration ( $\geq 1 \text{mM}$  ATP). Based on Michaelis–Menten fitting to our data obtained up to  $100 \mu\text{M}$  ATP, the maximum translocation rate of ScPif1 at saturating ATP concentration was estimated based on Michaelis–Menten fitting to be  $220.0 \pm 152.6$  nt/s, which is generally higher than the value  $\sim 80$  nt/s reported by previous bulk and single molecule studies (11,17). Although the cause of the higher translocation rate observed in our study is unclear, the force applied to the ssDNA in our single molecule manipulation could play a facilitating role. In a previous publication from our group, we reported that at forces below 6 pN, ssDNA tends to collapse into a compact conformation that could be due to hydrophobic base-stacking interaction or formation of other secondary structures (Figure 1 in (26)). In our double-hairpin assay, the translocation rate was measured at forces  $\sim 17$  pN where the ssDNA assumes an extended conformation without secondary structures formed inside. Therefore, it is likely that such an extended ssDNA conformation can reduce the kinetic barrier against the translocation of ScPif1, resulting in a faster translocation rate than that measured in previous bulk or smFRET assays where the ssDNA was not extended by force.

The observed repetitive helicase activity of ScPif1 in the double-hairpin assay after buffer washing indicates that the same ScPif1 could remain bound on the ssDNA and cause repetitive unwinding of the hairpin. While the mechanism behind is unclear, it is consistent with a previous single-molecule study that also reported repetitive unfolding of a hairpin by a single ScPif1 after buffer washing (12). One possible explanation to the repetitive activity of an ScPif1 helicase can be based on assuming that ScPif1 could ‘slip’ on the ssDNA, causing ScPif1 to slide backward (3′-to-5′) driven by the fork movement toward the direction of re-annealing. Another possibility is that during unwinding an ScPif1 could switch to the opposite strand and run in an opposite direction. Such ‘slipping’ and ‘strand-switching’ mechanisms have been suggested in previous studies for several helicases like Dda (30) and UvrD (31). Whether these mechanisms can also be applied to ScPif1 helicase activity warrants further investigations.

The mobile translocation mode may stand as a mechanism to boost ScPif1's helicase activity inside the cell. As shown in our data, this mode of translocation occurs frequently at low (nM range) concentrations, which allows ScPif1 molecules to bind any site of a ssDNA and swiftly move themselves in a 5'-to-3' direction to search for obstacle structures such as secondary DNA structures or proteins. The mechanism could lead to efficient enrichment of ScPif1 at the 5' side of a stable obstacle structure, promoting oligomerization of the ScPif1 enzymes. Previous studies have suggested that ScPif1 oligomerization could lead to a greater helicase capability that may help resolve the obstacle structure (9).

In the patrolling activity, we observed ScPif1-induced repetitive ssDNA shortening-extending dynamics that depends on ATP hydrolysis. The patrolling is surprisingly powerful. It can work against large forces up to 50 pN applied to the ssDNA. This force is significantly larger than the stall forces (typically <40 pN) of DNA polymerases and RNA polymerases (27,28). In addition, it is highly processive as indicated by the large loop sizes that can exceed 100 nt per run at forces above 10 pN. However, in spite of these interesting characteristics of the patrolling activity, the probability of its occurrence is much rarer than the mobile translocation at nM ScPif1 concentration. At higher concentrations, patrolling became more common. Although it remains unclear whether this patrolling mode of translocation plays a functional role in living cells, its powerful activity and its independence on anchoring to specific DNA structures provides it a potential capability of displacing obstacles at any location on ssDNA.

The data obtained in the patrolling mode of translocation reveal a trend that, the higher the force, the lower the looping rate as well as the loop size. The lowered looping rate can be qualitatively understood based on energy utilization - under force, the energy from ATP hydrolysis is not only needed for biased directional motion of ScPif1 motor domain on the ssDNA track, but also needed to compensate the energy cost of extension shortening against mechanical force. Thus, increased force is expected to slow down the translocation of the motor domain in the patrolling translocation mode. The force-dependent decrease in the loop size could also be understood by reasoning that the force may speed up the rate of disengagement of the motor domain from the ssDNA track.

The observed repetitive ssDNA shortening-extending behavior in the patrolling activity is similar to the previously reported ScPif1-dependent cyclic smFRET change of a DNA construct containing an ssDNA/dsDNA junction. That experiment has led to a mechanism of ScPif1 translocation activity, which assumes that the ScPif1 is anchored at an ssDNA/dsDNA junction, while its translocation domain travels along the ssDNA with a 5' to 3' direction. However, in our experiment, the patrolling was observed on ssDNA without any ssDNA/dsDNA junction. Therefore, the ssDNA/dsDNA junction is not necessary for such patrolling activity on ssDNA extended by mechanical force. In addition, we found that introducing an ssDNA/dsDNA junction did not significantly increase the chance to observe the patrolling; thus, the ssDNA/dsDNA junction seems not a promoting factor either under our experimen-

tal conditions. Whether these observations can be extended to situation where ssDNA is not extended by force warrants future investigations.

## CONCLUSION

Together, the results from this study provide new insights into our understanding of the ScPif1 translocation activity on ssDNA. Since the DNA duplex/G-quadruplex unwinding and protein displacement activities of ScPif1 all rely on the motor domain translocating on ssDNA, the two translocation modes of ScPif1 also shed light on the molecular mechanism behind these activities.

## SUPPLEMENTARY DATA

Supplementary Data are available at NAR Online.

## ACKNOWLEDGEMENTS

*Author contributions:* J.Y., K.D.R. and D.R. conceived the research. C.L., S.L and J.C. performed the experiments. C.L., S.L. and J.Y. analyzed the data. C.L. and J.Y. wrote the manuscript. A.K.B. purified the ScPif1 helicases. J.Y. and K.D.R. supervised the research.

## FUNDING

Singapore Ministry of Education under the Research Centres of Excellence programme (to J.Y.); Singapore Ministry of Education Academic Research Fund Tier 3 [MOE2012-T3-1-001 to J.Y. and D.R.]; Singapore Ministry of Education Academic Research Fund Tier 1 (to J.Y.); National Institutes of Health to the funding section [R35GM122601 to K.D.R.]. Funding for open access charge: Singapore Ministry of Education under the Research Centres of Excellence programme.

*Conflict of interest statement.* None declared.

## REFERENCES

- Lahaye,A., Stahl,H., Thines-Sempoux,D. and Foury,F. (1991) PIF1: a DNA helicase in yeast mitochondria. *EMBO J.*, **10**, 997–1007.
- Schulz,V.P. and Zakian,V.A. (1994) The Saccharomyces PIF1 DNA helicase inhibits telomere elongation and de novo telomere formation. *Cell*, **76**, 145–155.
- Zhou,J.-Q., Monson,E., Teng,S.-C., Schulz,V. and Zakian,V. (2000) Pif1p helicase, a catalytic inhibitor of telomerase in yeast. *Science*, **289**, 771–774.
- Zhang,D.-H., Zhou,B., Huang,Y., Xu,L.-X. and Zhou,J.-Q. (2006) The human Pif1 helicase, a potential Escherichia coli RecD homologue, inhibits telomerase activity. *Nucleic Acids Res.*, **34**, 1393–1404.
- Tran,P. L. T., Pohl,T.J., Chen,C.-F., Chan,A., Pott,S. and Zakian,V.A. (2017) PIF1 family DNA helicases suppress R-loop mediated genome instability at tRNA genes. *Nat. Commun.*, **8**, 15025.
- Budd,M.E., Reis,C.C., Smith,S., Myung,K. and Campbell,J.L. (2006) Evidence suggesting that Pif1 helicase functions in DNA replication with the Dna2 helicase/nuclease and DNA polymerase  $\delta$ . *Mol. Cell Biol.*, **26**, 2490–2500.
- Lahaye,A., Leterme,S. and Foury,F. (1993) PIF1 DNA helicase from Saccharomyces cerevisiae. Biochemical characterization of the enzyme. *J. Biol. Chem.*, **268**, 26155–26161.
- George,T., Wen,Q., Griffiths,R., Ganesh,A., Meuth,M. and Sanders,C.M. (2009) Human Pif1 helicase unwinds synthetic DNA structures resembling stalled DNA replication forks. *Nucleic Acids Res.*, **37**, 6491–6502.

9. Ramanagoudr-Bhojappa,R., Chib,S., Byrd,A.K., Aarattuthodiyil,S., Pandey,M., Patel,S.S. and Raney,K.D. (2013) Yeast Pif1 helicase exhibits a One-base-pair stepping mechanism for unwinding duplex DNA. *J. Biol. Chem.*, **288**, 16185–16195.
10. Singh,S.P., Koc,K.N., Stodola,J.L. and Galletto,R. (2016) A monomer of Pif1 unwinds double-stranded DNA and it is regulated by the nature of the non-translocating strand at the 3'-end. *J. Mol. Biol.*, **428**, 1053–1067.
11. Zhou,R., Zhang,J., Bochman,M.L., Zakian,V.A. and Ha,T. (2014) Periodic DNA patrolling underlies diverse functions of Pif1 on R-loops and G-rich DNA. *Elife*, **3**, e02190.
12. Li,J.-H., Lin,W.-X., Zhang,B., Nong,D.-G., Ju,H.-P., Ma,J.-B., Xu,C.-H., Ye,F.-F., Xi,X.G. and Li,M. (2016) Pif1 is a force-regulated helicase. *Nucleic Acids Res.*, **44**, 4330–4339.
13. Boule,J.-B. and Zakian,V.A. (2007) The yeast Pif1p DNA helicase preferentially unwinds RNA–DNA substrates. *Nucleic Acids Res.*, **35**, 5809–5818.
14. Sanders,C.M. (2010) Human Pif1 helicase is a G-quadruplex DNA-binding protein with G-quadruplex DNA-unwinding activity. *Biochem. J.*, **430**, 119–128.
15. Byrd,A.K. and Raney,K.D. (2015) A parallel quadruplex DNA is bound tightly but unfolded slowly by pif1 helicase. *J. Biol. Chem.*, **290**, 6482–6494.
16. Boulé,J.-B., Vega,L.R. and Zakian,V.A. (2005) The yeast Pif1p helicase removes telomerase from telomeric DNA. *Nature*, **438**, 57–61.
17. Galletto,R. and Tomko,E.J. (2013) Translocation of *Saccharomyces cerevisiae* Pif1 helicase monomers on single-stranded DNA. *Nucleic Acids Res.*, **41**, 4613–4627.
18. Sokoloski,J.E., Kozlov,A.G., Galletto,R. and Lohman,T.M. (2016) Chemo-mechanical pushing of proteins along single-stranded DNA. *Proc. Natl. Acad. Sci. U.S.A.*, **113**, 6194–6199.
19. Chen,H., Fu,H., Zhu,X., Cong,P., Nakamura,F. and Yan,J. (2011) Improved high-force magnetic tweezers for stretching and refolding of proteins and short DNA. *Biophys. J.*, **100**, 517–523.
20. Zhao,X., Zeng,X., Lu,C. and Yan,J. (2017) Studying the mechanical responses of proteins using magnetic tweezers. *Nanotechnology*, **28**, 414002.
21. Wenner,J.R., Williams,M.C., Rouzina,I. and Bloomfield,V.A. (2002) Salt dependence of the elasticity and overstretching transition of single DNA molecules. *Biophys. J.*, **82**, 3160–3169.
22. Fu,H., Chen,H., Zhang,X., Qu,Y., Marko,J.F. and Yan,J. (2010) Transition dynamics and selection of the distinct S-DNA and strand unpeeling modes of double helix overstretching. *Nucleic Acids Res.*, **39**, 3473–3481.
23. Presolski,S.I., Hong,V.P. and Finn,M. (2011) Copper-catalyzed azide–alkyne click chemistry for bioconjugation. *Curr. Protoc. Chem. Biol.*, **3**, 153–162.
24. Lu,K.-Y., Chen,W.-F., Rety,S., Liu,N.-N., Wu,W.-Q., Dai,Y.-X., Li,D., Ma,H.-Y., Dou,S.-X. and Xi,X.-G. (2017) Insights into the structural and mechanistic basis of multifunctional *S. cerevisiae* Pif1p helicase. *Nucleic Acids Res.*, **46**, 1486–1500.
25. Barranco-Medina,S. and Galletto,R. (2010) DNA binding induces dimerization of *Saccharomyces cerevisiae* Pif1. *Biochemistry*, **49**, 8445–8454.
26. Fu,H., Le,S., Chen,H., Muniyappa,K. and Yan,J. (2012) Force and ATP hydrolysis dependent regulation of RecA nucleoprotein filament by single-stranded DNA binding protein. *Nucleic Acids Res.*, **41**, 924–932.
27. Ibarra,B., Chemla,Y.R., Plyasunov,S., Smith,S.B., Lazaro,J.M., Salas,M. and Bustamante,C. (2009) Proofreading dynamics of a processive DNA polymerase. *EMBO J.*, **28**, 2794–2802.
28. Wang,M.D., Schnitzer,M.J., Yin,H., Landick,R., Gelles,J. and Block,S.M. (1998) Force and velocity measured for single molecules of RNA polymerase. *Science*, **282**, 902–907.
29. He,X., Byrd,A.K., Yun,M., Pemble IV,C.W., Harrison,D., Yeruva,L., Dahl,C., Kreuzer,K.N., Raney,K.D. and White,S.W. (2012) The T4 phage SF1B helicase Dda is structurally optimized to perform DNA strand separation. *Structure*, **20**, 1189–1200.
30. Byrd,A.K., Matlock,D.L., Bagchi,D., Aarattuthodiyil,S., Harrison,D., Croquette,V. and Raney,K.D. (2012) Dda helicase tightly couples translocation on single-stranded DNA to unwinding of duplex DNA: Dda is an optimally active helicase. *J. Mol. Biol.*, **420**, 141–154.
31. Dessinges,M., Lionnet,T., Xi,X.G., Bensimon,D. and Croquette,V. (2004) Single-molecule assay reveals strand switching and enhanced processivity of UvrD. *Proc. Natl. Acad. Sci. U.S.A.*, **101**, 6439–6444.
32. Bosco,A., Camunas-Soler,J. and Ritort,F. (2013) Elastic properties and secondary structure formation of single-stranded DNA at monovalent and divalent salt conditions. *Nucleic Acids Res.*, **42**, 2064–2074.
33. Marko,J.F. and Siggia,E.D. (1995) Stretching DNA. *Macromolecules*, **28**, 8759–8770.